CAVITY RING-DOWN SPECTROSCOPY OF O_2-O_2 COLLISIONAL INDUCED ABSORPTION

M. SNEEP and W. UBACHS
Laser Centre, Department of Physics and Astronomy, Vrije Universiteit, De Boelelaan 1081, 1081 HV Amsterdam, The Netherlands

Abstract. Absolute cross sections (peak and band-integrated) for collision-induced absorption features in oxygen at 630, 577 and 477 nm are determined using the laser-based technique of cavity ring-down spectroscopy. A wavelength-dependent background, Rayleigh scattering extinction and oxygen-monomer absorption are unraveled from the collision-induced features and its quadratic pressure dependence is demonstrated for sub-atmospheric pressures

Key words: Collision induced absorption, Oxygen, Cavity Ring-Down Spectroscopy

1. Introduction

The laser based-technique of cavity ring-down spectroscopy (CRDS) has in the past decade grown into an often used method for measuring absorption features of gas-phase molecules. Particularly when cavity mirrors of extreme reflectivity (i.e. exceeding 99.99%) are available, the sensitivity limit for detecting absorption is drastically improved. In this respect it challenges the alternative techniques of long-cell multi-pass Fourier-transform spectroscopy. Here we will describe some general characteristics of CRDS and report on cross section measurements of $(O_2)_2$ features. These collision-induced O_2-O_2 absorptions are associated with electronic resonances of primarily dissociative states, that play a role in the earth's atmosphere. They contribute to the radiation budget of the atmosphere for $\sim 1\mathrm{W/m}^2$ and these features with a quadratic pressure dependence can be used for determination of cloud tops in satellite remote sensing.

2. Principles of Cavity Ring-Down spectroscopy

The principle of CRDS is based upon a measurement of the rate of decay of an optical resonator with a high quality factor. It is schematically illustrated in figure

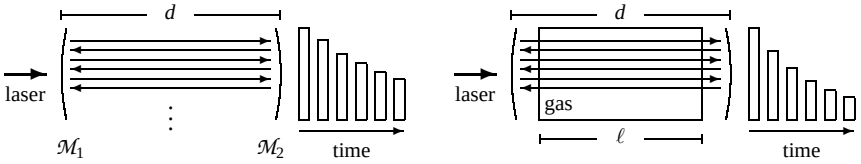

Figure 1. The principle of cavity ring-down

1. A laser pulse of short duration (usually 5 ns) is coupled into a stable but non-confocal cavity, consisting of two highly reflecting (typically $\mathcal{R} > 99.9\%$) curved mirrors. At each mirror a small part $(1-\mathcal{R})$ of the circulating power will be coupled out, while the remaining part is reflected back in the cavity. The first pulse leaking out of the cavity will have an intensity $I_0 = (1-\mathcal{R})^2 I_{\text{in}}$. The k^{th} pulse with intensity

$$\begin{aligned} I_k &= I_0 \mathcal{R}^{2(k-1)} \\ &= I_0 e^{2(k-1)\ln(\mathcal{R})} \end{aligned} \tag{1}$$

will leak out $(2d(k-1)n/c)$ seconds after the laser pulse, where c is the speed of light, n the index of refraction and d is the length of the cavity. Since we are dealing with gas-phase environments at low pressure the index of refraction is neglected. We will start with a cavity without absorbers.

A 5 ns pulse has a length of 1.5m. Practical ring-down cavities have a round-trip length ($2d$) of less than that, and therefore pulses will overlap inside the cavity. Furthermore the detection system usually has a response time that causes the discrete pulses to blend into a continuous signal as a function of time t,

$$I_{(t)} = I_0 e^{-(c/d)|\ln(\mathcal{R})|t} \tag{2}$$

Additional losses, usually caused by absorption of light or by Rayleigh scattering on molecules in the cavity, result in a faster decay. When the additional losses satisfy Beer's law, the decay remains exponential, yielding:

$$I_{(t)} = I_0 e^{-(c/d)\left(|\ln(\mathcal{R})|+\kappa_{(\nu)}\ell\right)t} \tag{3}$$

where ℓ is the length within the cavity that is filled with the absorbing species, see figure 1(b), and $\kappa_{(\nu)}$ the frequency dependent extinction coefficient.

The rate at which the ring-down signal decays with ($\beta_{(\nu)}$) or without ($\beta^0_{(\nu)}$) the presence of additional absorbers, is given by:

$$\beta_{(\nu)} = \frac{c\,|\ln(\mathcal{R})| + \kappa_{(\nu)}\ell}{d}; \quad \beta^0_{(\nu)} = \frac{c\,|\ln(\mathcal{R})|}{d} \tag{4}$$

From $\beta_{(\nu)}$ and $\beta^0_{(\nu)}$, we find an expression for the extinction induced by the medium, where we assume that the absorber fills the complete cavity, so $\ell = d$, yielding a simple equation for the extinction in terms of cavity decay rates.

$$\kappa_{(\nu)} = \frac{(\beta_{(\nu)} - \beta^0_{(\nu)})}{c} \tag{5}$$

The value $\beta^0_{(\nu)}/c$ is the background for the ring-down spectrum. This background is still frequency dependent because the mirror reflectivity depends on the frequency as well.

An important advantage of CRDS is the fact that the intensity of the light does *not* appear in equation 5; all information is contained in the time-evolution of the ring-down signal. The high sensitivity of CRDS is associated with this independence of the fluctuations of the light source. Another advantage is the fact that mirrors can now be made at such high reflectivity, up to $\mathcal{R} = 99.999\%$, that very long effective path lengths can be created, up to 100 km with a cavity length of only 80 cm. This leads to a very high sensitivity – absorptions as weak as 10^{-9} cm^{-1} can be detected.

A crucial issue is that the rate of decay of the cavity should be exponential. Only under that assumption the exponential decay associated with Beer's law for absorption can be added to the decay of the empty cavity (see Eq. 3) thus resulting in mono-exponential decay in a cavity filled with gas. If for some reason the resulting decay function is non-exponential no value of $\beta_{(\nu)}$ can be derived in the fitting procedure. Note that it is mathematically prohibited to design a fitting procedure to an arbitrary sum of exponentials. Multi-exponentiality can be caused by several mechanisms, the most common being laser-bandwidth induced effects. If the bandwidth of the exciting laser is non-negligible with respect to the width (Doppler or collisional) of the spectral line, then the various frequency components within the bandwidth profile are subject to different rates of absorption; hence these frequency components produce a sum of exponentials, which results in a non-exponential decay of the monitored signal. This effect is in fact the well-known "slit-function" problem of all spectroscopy, but its treatment, in the case of CRDS, is more complicated than usual because of its nonlinear nature. Although the problem has been noted in literature it still hampers the use of CRDS for the determination of absolute cross sections of narrow line features.

Another relevant issue for the analysis of ring-down transients is the proper treatment of the decay transients in fitting routines. As was elaborated by Naus *et al.* [4] a weighted non-linear least-squares fit to the data on the transient give the best determination of the decay life time, and in particular produces a reliable estimate of the uncertainty. As for the optical resonator it is important that it is aligned such that its mode structure does not result in wavelength-dependent effects. There is two methods for achieving this. In one method, developed by Van Zee *et al.* [7], the cavity is aligned in confocal position to transmit a sin-

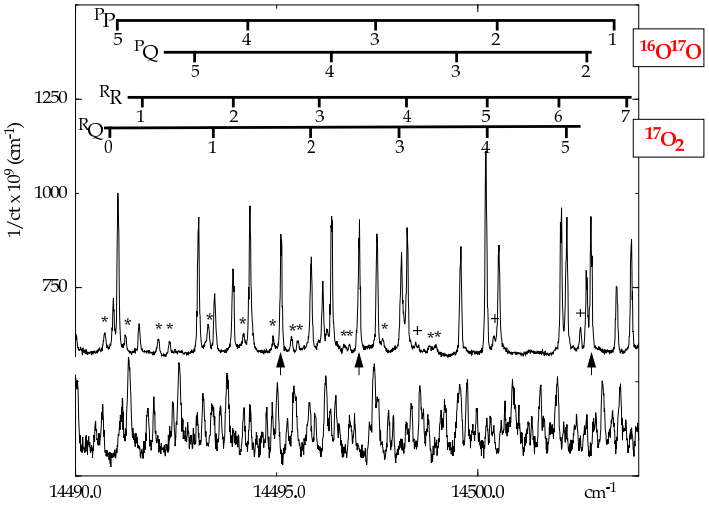

Figure 2. CRDS spectrum of the $b\,^1\Sigma_u^+ \leftarrow X\,^3\Sigma_g^-(1,0)$ or B-band of oxygen for a (50% atom) ^{17}O enriched sample, measured at a pressure of 16.5 Torr. Lines pertaining to $^{16}O^{17}O$ and $^{17}O_2$ are assigned, while the lines marked with $*$, $+$ and $\uparrow$ belong to $^{17}O^{18}O$, $^{16}O^{18}O$ and $^{16}O_2$ respectively. The lower panel shows a simultaneously recorded I_2 spectrum, used for calibration.

gle mode adapted to the laser frequency. Although the method yields accurate results it is not well-suited to be used in absorption measurements, where fairly large wavelength ranges are to be scanned. In the alternative method the cavity is aligned far from confocal ($d \approx 0.85 r_c$, d the distance between the mirrors and r_c the radius of curvature), such that a large number of longitudinal and transversal cavity modes is supported, making the cavity a white light transmitter. It is noted that in this condition only a very small fraction ($[1-\mathcal{R}]^2$) of the initial laser pulse reaches the detector. The optical resonator then acts as a white-light filter and the configuration can be used for wavelength-scanning pulsed CRDS. The relation between mode-structure and transmission, and an experimental method to improve alignment towards single-exponential decay in a non-confocal resonator were discussed in reference [4].

3. Measurements on small samples

As was mentioned in the introduction, both CRDS and Fourier-transform spectroscopy, have developed into sensitive tools for direct absorption measurements. An unambiguous general statement as to the sensitivity of either technique cannot be made, because in CRDS the sensitivity strongly depends on the reflectivity of the mirrors available, while for FT-spectroscopy the sensitivity depends on the geometrical configuration of an absorption path connected to the spectrometer. We mention here that CRDS lacks the so-called multiplex advantage of

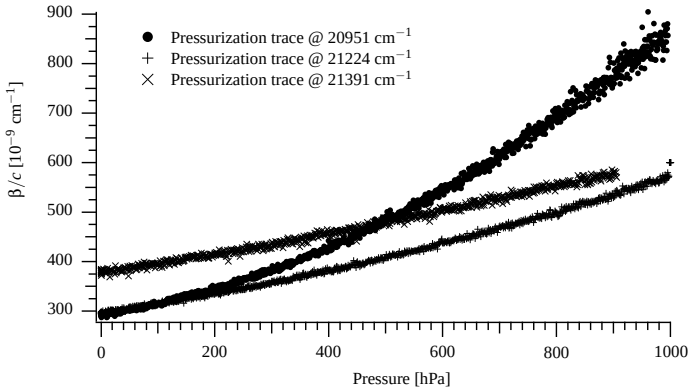

Figure 3. Three typical pressurization traces. The offset $\beta^0_{(\nu)}/c$ on the vertical axis shows the difference in mirror reflectivity between the three frequency positions.

FT-spectroscopy: data have to be collected at each wavelength position, making the technique time consuming. One noteworthy advantage of CRDS is that a high sensitivity can be obtained from a compact setup, in which only small amounts of gas are required. This is a particularly useful property for the spectroscopic investigation on isotopically enriched samples, which are only available in small amounts. This is demonstrated in figure 2 for measurements of the B-band of molecular oxygen, published before in [3]. The spectral recording is taken from a 50% oxygen-17 enriched sample of oxygen in a cell of 1 cm diameter and 40 cm length.

4. CRD measurements of oxygen collisional complexes

As a result of the binding properties between two ground state oxygen atoms $O(^3P) + O(^3P)$ there are several low-lying electronic states in the O_2 molecule. However, all possible transitions between these molecular states are, in the electric dipole approximation, forbidden by quantum selection rules. During a collision some of these transitions are allowed and absorption of a photon can occur. The collision pair does not have to be bound and each of the molecules caries away part of the photon energy. Since the number of collision pairs is proportional to the square of the density, the strength of the absorption also increases with the square of the density.

To measure the absorption strength of the oxygen collision complexes, one could scan over the absorption feature at various pressures. A better separation between the background $\beta^0_{(\nu)}/c$ – determined by the mirrors and how well they are cleaned, a component with a linear density dependence – Rayleigh scattering, and a component with a quadratic density dependence can be obtained by scanning the density, while maintaining the laser at a fixed frequency. The loss rate as a

function of density $\tilde{n}$ is:

$$\beta_{(\nu)}(\tilde{n}) = \beta^0_{(\nu)} + \sigma^R \tilde{n}\, c + \alpha^q \tilde{n}^2\, c \tag{6}$$

where σ^R is the Rayleigh scattering cross section and α^q is the collisional induced absorption cross section.

While oxygen was slowly flushed into the ring-down cavity, the loss-rate $\beta_{(\nu)}(\tilde{n})$ was constantly monitored by a 10 Hz pulsed laser. The pressure ramp spans a range of 0 to 1000 hPa and consists of about 1100 measurements of $\beta_{(\nu)}$. To obtain a spectrum of the entire resonance, the laser is tuned to a different frequency and the procedure is repeated. Three typical pressurization traces can be found in figure 3. The parameters of Eq. 6 are fitted to the measured data. The Rayleigh scattering cross section can be calculated from the refractive index and the depolarization ratio. In the final fit, σ^R is fixed to this value.

An explicit advantage of the pressure-ramp method is that at each wavelength position the contributions of baseline, linear extinction and the true collisional-induced quadratic feature can be unraveled in a fitting routine. Extraction of the baseline is crucial if the goal is to derive a cross-section of an absorption feature. Since a major part of the cross-section is near the baseline, the slightest mis-judgment of the background causes a strong deviation in the cross-section. In a scanning experiment baseline fluctuations can be interpreted as absorption signal. Note that Newnham *et al.* [5] had to set the baseline to zero at two frequency positions, adding a source of systematic uncertainty, which is avoided in the pressure ramp method.

Another issue is that wavelength positions for pressure ramp scans can be carefully chosen. In the case of the red collisionally induced feature at 630 nm there is oxygen monomer absorption (the γ-band) overlaying the collision-induced feature. The contribution of the monomer and collision feature could be unraveled

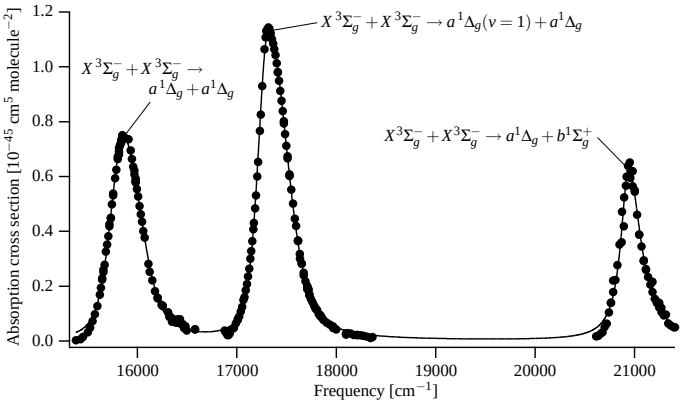

Figure 4. The three visible O_2-O_2 absorption features near 630, 577 and 477 nm. The transitions are indicated in the graph. For all transitions $v = 0$, unless indicated otherwise.

TABLE I. An overview of the literature value of the $(O_2)_2$ transitions. The values in parentheses are 1σ uncertainties.

ref	position [cm^{-1}]	width [cm^{-1}]	height [10^{-46} cm^{-5} $molecule^{-2}$]	integral [10^{-43} cm^{-4} $molecule^{-2}$]
$[a\,^1\Delta_g(v=0)]_2 \leftarrow [X\,^3\Sigma_g^-(v''=0)]_2$ at 630 nm				
[1]	15869 (5)	368 (5)	7.2 (2)	3.1 (1)
[5]	15862 (5)	369 (5)	7.1 (2)	2.8 (1)
[2]	15880 (1)	367 (1)	7.55 (5)	3.19 (3)
$[a\,^1\Delta_g(v'=0)+a\,^1\Delta_g(v'=1)] \leftarrow [X\,^3\Sigma_g^-(v''=0)]_2$ at 577 nm				
[1]	17320 (5)	348 (5)	11.0 (3)	4.8 (1)
[5]	17314 (5)	339 (5)	11.7 (3)	4.7 (1)
[2]	17308 (1)	340 (1)	11.41 (5)	4.66 (3)
$[b\,^1\Sigma_g^+(v'=0)+a\,^1\Delta_g(v'=0)] \leftarrow [X\,^3\Sigma_g^-(v''=0)]_2$ at 477 nm				
[1]	20951 (5)	270	6.3 (6)	—
[5]	20951 (5)	—	8.34 (83)	2.483 (48)
[6]	20930 (2)	241 (7)	6.38 (16)	2.18 (4)

by choosing wavelengths in between rotational absorption lines in the $b\,^1\Sigma_g^+(v=2) \leftarrow X\,^3\Sigma_g^-$ band of $^{16}O_2$ for the construction of the line profile of the broad $[a\,^1\Delta_g(v=0)]_2 \leftarrow [X\,^3\Sigma_g^-(v=0)]_2$ collision feature.

Finally we note that effects of non-exponential behaviour were not present in the study of these O_2-O_2 features. The CRDS cavity was carefully aligned towards a condition of purely exponential decay. Moreover laser-bandwidth effects do not play a role: it is below 0.1 cm^{-1}, while the width of the oxygen resonances exceeds 100 cm^{-1}.

In figure 4 an overview is given of three of the visible O_2-O_2 absorption features. Black points represent the quadratic component derived from a pressure ramp scan. The features $[a\,^1\Delta_g(v=0)]_2 \leftarrow [X\,^3\Sigma_g^-(v=0)]_2$ at 630 nm and $[a\,^1\Delta_g(v=0)+a\,^1\Delta_g(v=1)] \leftarrow [X\,^3\Sigma_g^-(v=0)]_2$ at 577 nm are described in reference [2], the $[b\,^1\Sigma_g^+(v=0)+a\,^1\Delta_g(v=0)] \leftarrow [X\,^3\Sigma_g^-(v=0)]_2$ feature near 477 nm is described in reference [6]. In this frequency range another feature exists near 532 nm; an overview of the other O_2-O_2 transitions can be found in reference [1].

The data in table I was measured using various methods: Greenblatt *et al.* [1] used a cell at 55 atmosphere. Newnham *et al.* [5] employed a long path FT spectrometer, recording the spectrum at 1000 hPa. Extraction of the quadratic pressure dependence was done from this single pressure alone. In their conclusions it is

specifically mentioned that more measurements at a lower pressure are needed for the O_4 absorption bands. An important result of the present CRDS data is, that it is established that the quadratic behaviour and the pressure dependent cross sections also hold for sub-atmospheric pressures.

References

1. Greenblatt, G. D., J. J. Orlando, J. B. Burkholder, and A. R. Ravishankara: 1990, 'Absorption Measurements of Oxygen between 330 and 1140 nm'. *J. Geophys. Res.* **95**(D11), 18577–18582.
2. Naus, H. and W. Ubachs: 1999, 'Visible absorption bands of the $(O_2)_2$ collision complex at pressures below 760 Torr'. *Appl. Opt.* **38**(15), 3423.
3. Naus, H., S. J. van der Wiel, and W. Ubachs: 1998, 'Cavity-Ring-Down Spectroscopy on the $b\,^1\Sigma_g^+ - X\,^3\Sigma_g^-(1,0)$ Band of Oxygen Isotopomers'. *J. Mol. Spectr.* **192**, 162–168.
4. Naus, H., I. H. M. van Stokkum, W. Hogervorst, and W. Ubachs: 2001, 'Quantitative analysis of decay transients applied to a multimode pulsed cavity ringdown experiment'. *Appl. Opt.* **40**(24), 4416–4426.
5. Newnham, D. A. and J. Ballard: 1998, 'Visible absorption cross sections and integrated absorption intensities of molecular oxygen (O_2 and O_4)'. *J. Geophys. Res.* **103**(D22), 28801–28816.
6. Sneep, M. and W. Ubachs: 2003, 'Cavity Ring-Down Measurements of the O_2-O_2 collision induced absorption resonance at 477 nm at sub-atmospheric pressures'. *J. Quant. Spectrosc. Radiat. Transfer*. Accepted for publication.
7. Van Zee, R. D., J. T. Hodges, and J. P. Looney: 1999, 'Pulsed, single-mode cavity ringdown spectroscopy'. *Appl. Opt.* **38**(18), 3951.